Analytical theory of coherent radiation and radiation friction in laser-plasma collisions

E. G. Gelfer,[1,*] A. M. Fedotov,[2,3] M. P. Malakhov,[2,4] Th. Benahmed,[1,†] J. Custodio,[1,5] O. Klimo,[1,5] and S. Weber[1]

[1]*ELI Beamlines facility, The Extreme Light Infrastructure ERIC, Dolni Brezany 252 41, Czech Republic*
[2]*Department of Theoretical Nuclear Physics, National Research Nuclear University MEPhI, Moscow 115409, Russia*
[3]*Institute of Applied Physics of the Russian Academy of Sciences, Nizhny Novgorod 603950, Russia*
[4]*Skolkovo Institute of Science and Technology, Skolkovo 121205, Russia*
[5]*FNSPE, Czech Technical University in Prague, Prague, Czech Republic*

(Received 5 May 2026; accepted 30 June 2026; published 27 August 2026; corrected 21 October 2026)

We develop an analytical theory of coherent (scaled quadratically with the number of particles) radiation and coherent radiation friction in a head-on collision of a dense charged particle bunch with an intense laser pulse. We demonstrate that the low-frequency coherent radiation in the forward and backward directions dominates the energy-momentum losses of a mildly relativistic bunch and can result in a substantial enhancement of the overall radiation friction as compared to the incoherent case. We derive the scaling laws for the average momentum losses of the bunch over the collision with respect to laser intensity, pulse duration, and particle bunch parameters, and show their robustness with respect to laser polarization and the shape of the particle distribution in the bunch.

DOI: 10.1103/wv25-1w9h

I. INTRODUCTION

When charged particles collide with a laser pulse, they emit electromagnetic radiation losing energy and momentum. From classical viewpoint, this effect, conventionally called radiation reaction or radiation friction (RF) [1–3], can be formally described by introducing a RF force $\mathbf{F}_{\rm RF}$ into the equation of motion,

$$\frac{d\mathbf{p}}{dt} = \mathbf{F}_L + \mathbf{F}_{\rm RF}, \tag{1}$$

where $\mathbf{F}_L = e(\mathbf{E} + [\mathbf{v} \times \mathbf{B}]/c)$ is the Lorentz force; $\mathbf{E}$ and $\mathbf{B}$ are the electric and magnetic fields; e, $\mathbf{p}$ and $\mathbf{v}$ are the charge, momentum, and velocity of the particle.

RF has been recently observed experimentally in laser-particles collisions [4–6] and it is foreseeable that RF can be important in practical applications of strong laser-plasma interaction, such as electron and ion acceleration [7–15], generation of waves in a rarefied plasma [16,17], or strong magnetic fields in a dense plasma [18,19]. It also modifies the spectrum of radiation itself [20–23].

Assuming $B \sim E$, classical description is valid as long as the quantum parameter $\chi \sim \frac{\gamma E}{E_{\rm cr}}$, which measures the ratio of the electric field in the particle rest frame to the critical field of quantum electrodynamics (QED) $E_{\rm cr} = m^2c^3/e\hbar$ [24,25], is small [26,27]. Here m and γ are the particle mass and Lorentz factor. In what follows, we assume the classical regime $\chi \ll 1$ of radiation and radiation friction.

Several expressions for the RF force have been proposed in the literature [1,2,28,29]; see also the review in Ref. [30]. The one introduced by Landau and Lifshitz (LL) [2] is now commonly accepted as a convenient approximation for the description of RF in the classical regime [31,32].

It is conventionally believed that RF is relevant in interactions of ultraintense lasers with ultrarelativistic particles; see the reviews [27,30–32]. Indeed, according to the estimates [9,20] based on the LL approach, RF is substantial for

$$\mathcal{R} = \mu a_0^2 \gamma \omega_L T \gtrsim 1, \quad \mu = \frac{4\pi}{3}\frac{r_e}{\lambda_L}, \tag{2}$$

where $a_0 = eE_0/m\omega_L c$ is the amplitude of the dimensionless field strength; ω_L, λ_L, and T are the frequency, wavelength, and duration of the laser pulse; and $r_e = e^2/mc^2 \approx 2.8 \times 10^{-13}$ cm is the classical electron radius. For an optical petawatt class laser $\mu \sim 10^{-8}$, $\omega_L T \sim 10 - 100$, so that Eq. (2) can be satisfied only for $a_0 \gg 1$ and/or $\gamma \gg 1$.

However, Eq. (1) and the condition equation (2) have been derived under the assumption that the particles emit radiation independently and incoherently. This assumption might not be fulfilled for a dense particle bunch [33–36]. Since the energy of the emitted coherent radiation scales with the number of radiating particles N as N^2 [33–43], the coherence can strongly enhance RF.

Here we investigate coherently enhanced RF in a head-on collision of a charged particle bunch with a plane wave laser pulse. We provide a detailed derivation of the analytical theory of the effect and demonstrate its robustness with respect to the models in use for the laser pulse and the particle bunch.

In the companion Letter [44] we summarize the main physical results, provide their numerical validation with three-dimensional particle-in-cell (PIC) simulations, confront the

*Contact author: egelfer@gmail.com
†Present address: Deutsches Elektronen–Synchrotron DESY, Notkestr. 85, 22607 Hamburg, Germany.

Published by the American Physical Society under the terms of the Creative Commons Attribution 4.0 International license. Further distribution of this work must maintain attribution to the author(s) and the published article's title, journal citation, and DOI.

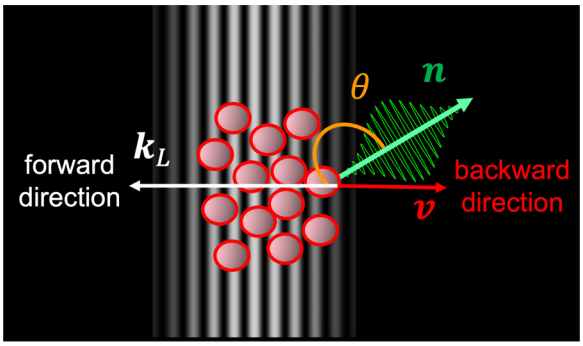


FIG. 1. Illustration of the laser-bunch collision geometry; $\mathbf{k}_L$—laser wave-vector; $\mathbf{v}$—velocity of the particles; $\mathbf{n}$—direction of radiation.

coherently enhanced RF with the ordinary incoherent one, and discuss the prospects for experimental observation of coherent RF in such a setup.

The paper is organized as follows. In Sec. II we derive an analytical approximation for the radiation spectrum of a bunch of charged particles. To this end we follow the approach of Ref. [35] but, whereas there the main focus was on the high-frequency part of the radiation spectrum, here we mostly consider radiation at small frequencies, which contributes most to the energy and momentum transfer in the regime of coherently enhanced RF. In Sec. III we derive an amount of momentum lost on average by a particle in a dense bunch. First we discuss the known result for a single particle, then calculate the momentum losses assuming the coherent radiation is dominant. In Sec. IV we discuss the obtained analytical results with an emphasis on their robustness with respect to the laser polarization and the bunch shape. Section V summarizes our findings. The Appendix supports the discussion of Sec. IV by providing a detailed calculation of RF for an alternative bunch shape.

II. RADIATION OF A PARTICLE BUNCH COLLIDING WITH A LASER PULSE

We start with a general formula for the radiation emitted by a bunch of N particles colliding with a laser pulse; see Fig. 1. Assuming the waist w of the laser pulse is much larger than both the laser wavelength and the radius of the bunch, $w \gg \lambda_L,\ R$ we consider the laser pulse as a plane wave pulse propagating along x axis, for which the vector potential $\mathbf{A}(\phi)$ depends solely on its phase $\phi = \omega_L(t - x/c)$ (ω_L is the laser frequency). Then it is convenient to parametrize particle trajectories and momenta by the phases $\phi_j = \omega_L(t - x_j/c)$, where j ($1 \leqslant j \leqslant N$) labels the particles. In these terms the angular-frequency distribution of the radiation can be written in the form [3]

$$\frac{d\mathcal{E}}{d\omega d\Omega} = \frac{\omega^2}{4\pi^2\omega_L^2 c} \times \left| \sum_{j=1}^{N} \frac{e_j}{p_{-,j}} \int [\mathbf{n} \times [\mathbf{n} \times \mathbf{p}_j(\phi_j)]] e^{i\omega \varkappa(\phi_j)} d\phi_j \right|^2, \tag{3}$$

where $\varkappa(\phi_j) = \phi_j/\omega_L + [x_j(\phi_j) - \mathbf{n}\mathbf{r}_j(\phi_j)]/c$; $\mathbf{n}$ and ω are the direction and frequency of the emitted radiation; e_j, $\mathbf{r}_j(\phi_j)$, and $\mathbf{p}_j(\phi)$ are the charge, coordinates, and momenta of the jth particle of the bunch; and $p_- = \gamma mc - p_x$ is the light-front momentum conserved along the trajectory in a plane wave field.

A. Initial phase of a particle in a bunch

Consider the trajectories of particles colliding head on with a plane wave laser pulse. Assuming the same initial momenta of all the particles [45], it follows from the equation of motion without RF that the phase dependence of the particle momenta is the same for all particles,

$$\mathbf{p}_j(\phi_j) \equiv \mathbf{p}(\phi_j). \tag{4}$$

Next, from $d\mathbf{r}_j/d\phi_j = c\mathbf{p}/\omega_L p_-$ we obtain

$$\mathbf{r}_j = \mathbf{r}_j(\hat{\phi}) + \mathbf{r}(\phi_j), \quad \mathbf{r}(\phi_j) = \int_{\hat{\phi}}^{\phi_j} \frac{c\mathbf{p}(\phi')}{\omega_L p_-} d\phi', \tag{5}$$

where $\hat{\phi}$ is a (common for all the particles) initial value of the phase.

By substituting Eqs. (4) and (5) into Eq. (3) we find that Eq. (3) can be factorized [33,35,46],

$$\frac{d\mathcal{E}}{d\omega d\Omega} = \mathcal{C}\frac{d\mathcal{E}^{(1)}}{d\omega d\Omega}, \quad \mathcal{C} = \left| \sum_{j=1}^{N} e^{i\Phi_j} \right|^2, \tag{6}$$

where $d\mathcal{E}^{(1)}/d\omega d\Omega$ is the single-particle radiation spectrum corresponding to Eq. (3) with $N = 1$ and $\Phi_j = \omega[x_j(\hat{\phi}) - \mathbf{n}\mathbf{r}_j(\hat{\phi})]/c$.

For practical reasons it is more convenient to express the phase shifts Φ_j of the particles through their initial positions $\mathbf{r}_j^0 \equiv \mathbf{r}_j[\phi_j(t_0)]$ at a given common time t_0 rather than $\mathbf{r}_j(\hat{\phi})$ at a common phase. Let us choose the initial time t_0 such that all the particles are still outside the pulse moving freely with the initial momentum $p_x = -p_0$; i.e., $x_j(\phi) = x_j(\hat{\phi}) - p_0(\phi - \hat{\phi})/\omega_L p_-$. Then up to a common constant term we have

$$x_j(\hat{\phi}) = x_j^0\left(1 - \frac{p_0}{p_-}\right) + \frac{p_0 t_0}{p_-}, \quad \mathbf{r}_{\perp,j}(\hat{\phi}) = \mathbf{r}_j^0. \tag{7}$$

Finally, taking into account that in the relativistic case $p_0 \approx p_-/2$, from Eq. (7) we arrive at

$$\Phi_j = \omega[(1 - \cos\theta)x_j^0/2 - \mathbf{n}_\perp \mathbf{r}_{j,\perp}^0]/c. \tag{8}$$

Here x_j^0, $\mathbf{r}_{j,\perp}^0$ are the particle initial longitudinal and transverse coordinates.

Note that the factor $1/2$ in the longitudinal contribution was missed in previous works [33,35]. It appears due to the fact that the laser pulse propagates toward the particles and does not appear in a static field, e.g., for synchrotron radiation [46].

B. Coherent and incoherent contributions

Consider now factor $\mathcal{C}$ that relates single- and multiple-particle spectra in Eq. (6). Representing $\mathcal{C} = \sum_{j,k} e^{i(\Phi_j - \Phi_k)}$

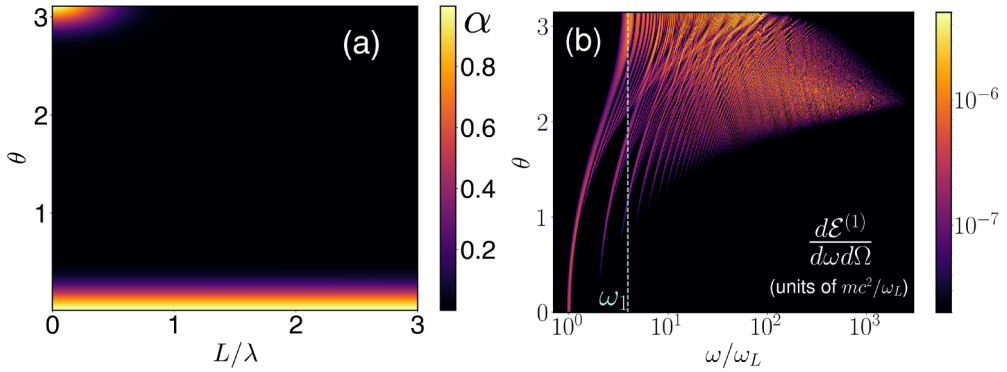


FIG. 2. Coherence factor (a) and radiation spectrum of a single particle (b) for a head-on collision of electrons with a plane wave laser pulse; ω_1 is the fundamental harmonic of the backward radiation defined in Eq. (21); $R = \lambda$, $p_0 = 5mc$, $T \approx 50$ fs.

and decomposing the sum to N diagonal and $N(N-1)$ off-diagonal terms [46] we get

$$\mathcal{C} = N(1-\alpha) + N^2\alpha, \tag{9}$$

where $\alpha = |\langle e^{i\Phi}\rangle|^2$ is the modulus squared average of the particle initial phase factor. The terms $N(1-\alpha)$ and $N^2\alpha$ correspond to the incoherent and coherent parts of the radiation, respectively. The second (coherent) term is dominant for $\alpha N \gg 1$. In what follows we will call α the coherence factor.

For a given initial density distribution $n(\mathbf{r^0})$ of particles in a bunch the coherence factor α can be calculated as

$$\alpha = \left|\frac{1}{N}\int n(\mathbf{r^0})e^{i\Phi(\mathbf{r^0})}d\mathbf{r}^0\right|^2, \tag{10}$$

where $N = \int n(\mathbf{r^0})d\mathbf{r}^0$. In particular, for a Gaussian density distribution $n(x, \mathbf{r}_\perp) = n_0 \exp(-\frac{x^2}{(L/2)^2} - \frac{r_\perp^2}{R^2})$ employed in Ref. [44] we have

$$\alpha = e^{-\frac{\omega^2}{8c^2}\left(L^2\sin^4\frac{\theta}{2} + 4R^2\sin^2\theta\right)}. \tag{11}$$

It is worth noting that $\alpha \approx 1$ for a small bunch such that $R, L \ll \lambda$, where $\lambda = 2\pi c/\omega$ is the wavelength of the emitted radiation. This means that the radiation is fully coherent in all directions and N particles of charge e can be replaced with a single particle of charge Ne. If R and/or $L \gtrsim \lambda$, then α has a global maximum $\alpha = 1$ at $\theta = 0$ (forward radiation) and, depending on R and L, an additional peak at $\theta = \pi$ (backward radiation). It is easy to see that in the Gaussian case this additional peak appears if $L < 2\sqrt{2}R$. However, for $L \gg \lambda$ its contribution is strongly suppressed; see Fig. 2(a).

C. Single-particle radiation in forward and backward directions

According to Eqs. (6) and (9), the N-particle spectrum is a product of the coherence factor (10) and the single-particle spectrum $d\mathcal{E}^{(1)}/d\omega d\Omega$. While the coherence factor can be calculated analytically at least for simple shapes of the particle bunch, the single-particle spectrum in a finite laser pulse in general has to be evaluated numerically [47–49]; see the result of such evaluation in Fig. 2(b).

However, as shown above, see also Ref. [44], for a large bunch (of size larger than the emitted wavelength at least in one dimension), the coherent radiation narrowly peaks around the backward and/or forward direction. Therefore, for analytical evaluation of the coherent radiation spectrum, it is enough approximate the single-particle spectrum in these directions, where it can be cast in the form [35,50]

$$\left.\frac{d\mathcal{E}^{(1)}}{d\omega d\Omega}\right|_{\theta=0,\pi} = \frac{e^4\omega^2}{4\pi^2 c\omega_L^2 p_-^2}\left|\int \mathbf{A}(\phi)e^{\frac{i\omega}{\omega_L}(\phi+\upsilon(\phi))}d\phi\right|^2, \tag{12}$$

where $\upsilon(\phi) = 0$ for $\theta = 0$ (forward radiation) and $\upsilon(\phi) = 2\omega_L x(\phi)/c$ for $\theta = \pi$ (backward radiation). Here

$$x(\phi) = \frac{c}{\omega_L}\left[\frac{p_\parallel}{p_-}\phi + \frac{m^2c^2}{2p_-^2}\int_{-\infty}^{\phi}\hat{\mathbf{A}}^2(\psi)d\psi\right]$$

is the longitudinal coordinate of the particle and $\hat{\mathbf{A}}(\phi) = e\mathbf{A}(\phi)/mc$ is the dimensionless vector potential.

In particular, the forward radiation spectrum is proportional to the spectrum of the incident laser pulse. For an incoming circularly polarized pulse of duration T with a Gaussian temporal envelope,

$$\mathbf{A} = \frac{mca_0}{e}e^{-\phi^2/(\omega_L T)^2}\{0, \cos\phi, \sin\phi\}, \tag{13}$$

the forward scattered spectrum,

$$\left.\frac{d\mathcal{E}^{(1)}}{d\omega d\Omega}\right|_{\theta=0} \approx \frac{e^2\omega^2T^2}{8\pi c}\frac{m^2a_0^2c^2}{p_-^2}e^{-\frac{(\omega-\omega_L)^2T^2}{2}}, \tag{14}$$

is also Gaussian, centered at the laser carrier frequency ω_L.

For the backscattered radiation we have

$$\left.\frac{d\mathcal{E}^{(1)}}{d\omega d\Omega}\right|_{\theta=\pi} = \frac{e^2p_-^2\zeta^2}{4\pi^2m^2c^3}\left|\int \hat{\mathbf{A}}(\phi)e^{if(\phi)}d\phi\right|^2,$$
$$f(\phi) = \zeta\left(\phi + \int_{-\infty}^{\phi}\hat{\mathbf{A}}^2(\psi)d\psi\right), \tag{15}$$

where $\zeta = (mc/p_-)^2\omega/\omega_L$. The integral in Eq. (15) can be evaluated by the stationary phase approximation [35,51,52].

Representing Eq. (13) in terms of complex exponentials, we observe that for a long pulse $\omega_L T \gg 1$ each of the phases $if(\phi) \pm i\phi$ in Eq. (15) has two stationary points,

$$\phi_\pm^1 = \pm\omega_L T\sqrt{\frac{1}{2}\ln\frac{\zeta a_0^2}{1-\zeta}}, \tag{16}$$

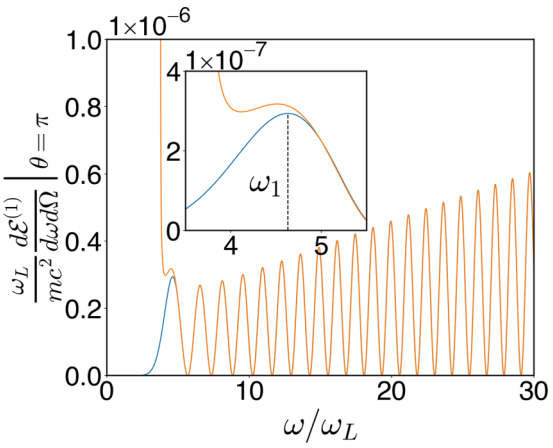


FIG. 3. Single-particle radiation spectrum in backward direction evaluated numerically (blue) and its analytical approximation Eq. (19) (orange). Other parameters: $a_0 = \gamma_0 = 5$, $T = 67$ fs, $\lambda_L = 1$ μm. Inset: the same plot zoomed in near the first maximum ω_1.

and

$$\phi_\pm^2 = \pm\omega_L T\sqrt{\frac{1}{2}\ln\frac{\zeta a_0^2}{-1-\zeta}}. \tag{17}$$

Since for all real ζ the points $\phi_\pm^2$ are imaginary and such that $|\mathrm{Im}\phi_\pm^2| > |\mathrm{Im}\phi_\pm^1|$, their contribution is exponentially suppressed and can be neglected. In contrast, stationary points (16) are real in the range $1/(1+a_0^2) < \zeta < 1$, which corresponds to

$$\hat{\omega} = \frac{p_-^2\omega_L}{m^2c^2(1+a_0^2)} < \omega < \frac{p_-^2\omega_L}{m^2c^2} = \omega_*. \tag{18}$$

Outside the range (18), in particular, for $\omega > \omega_*$, all the saddle points are purely imaginary and the radiation spectrum falls out exponentially. Such high frequencies are, however, irrelevant to the coherent effects of our primary interest here.

Applying the standard formula for the stationary phase approximation, we arrive at

$$\left.\frac{d\mathcal{E}^{(1)}}{d\omega d\Omega}\right|_{\theta=\pi} \approx \frac{e^2}{4\pi c}\frac{\omega T}{\nu}(1+\sin\eta), \quad \hat{\omega} < \omega \ll \omega_*, \tag{19}$$

where

$$\eta = \frac{\omega_L T}{2\omega_*}\left[2\nu(\omega-\omega_*) + \sqrt{2\pi}a_0^2\omega\,\mathrm{erf}\left(\frac{\nu}{\sqrt{2}}\right)\right],$$
$$\nu = \sqrt{2\ln\frac{\omega a_0^2}{\omega_*-\omega}}, \tag{20}$$

and $\mathrm{erf}(z) = (2/\sqrt{\pi})\int_0^z e^{-\zeta^2}d\zeta$ is the error function.

Approximation (19) is compared to the numerically evaluated backward radiation spectrum in Fig. 3. It is seen that this approximation works reasonably well to the right of $\hat{\omega}$, where it diverges because the saddle points ϕ_+^1 and ϕ_-^1 merge at the origin, making the second derivative of the phase vanishing. Nevertheless, Eq. (19) still remains reasonably accurate even at $\omega = \omega_1$, the position of the first maximum of the spectrum (see the inset in Fig. 3); hence it can be used to estimate ω_1.

To this end we write $\omega_1 = \hat{\omega}(1+\delta)$ assuming $\delta \ll 1$ and require $\eta(\omega_1) = \frac{\pi}{2}$, where $\eta(\omega)$ is introduced in Eq. (20). A straightforward calculation gives

$$\delta \approx \frac{1}{2}\left(\frac{3\pi}{2\omega_L T}\right)^{2/3}, \tag{21}$$

and it is seen that the implied assumption $\delta \ll 1$ indeed holds for $\omega_L T \gg 1$.

Finally, from Eq. (21) in the same approximation $\omega_L T \gg 1$ we obtain

$$\omega_1 \approx \omega_L\xi^2\left[1+\frac{1}{2}\left(\frac{3\pi}{2\omega_L T}\right)^{2/3}\right], \tag{22}$$

and, by virtue of Eq. (19),

$$\left.\frac{d\mathcal{E}^{(1)}}{d\omega d\Omega}\right|_{\theta=\pi,\omega=\omega_1} \approx \frac{e^2}{c}\frac{3\xi^2}{4}\left(\frac{2\omega_L T}{3\pi}\right)^{4/3}, \tag{23}$$

where $\xi = \frac{p_-}{mc\sqrt{1+a_0^2}}$.

D. Coherent radiation of a particle bunch

At this point, we approximate the angular-frequency distribution of the coherent radiation of the particle bunch by

$$\frac{d\mathcal{E}_{\mathrm{coh}}}{d\omega d\Omega} \approx \alpha N^2 \left.\frac{d\mathcal{E}^{(1)}}{d\omega d\Omega}\right|_{\theta=0,\pi}, \tag{24}$$

where the coherence factor is defined in Eq. (10) and we replace the exact single-particle spectrum with the spectrum equation (14) of forward scattering for $0 \leqslant \theta < \pi/2$ and with the spectrum equation (19) of backward scattering for $\pi/2 < \theta \leqslant \pi$.

Comparing the approximation equation (24) with Eq. (6), where the single-particle spectrum is evaluated numerically, as in Fig. 2(b), we find that they match very well [53]; see Fig. 4. As discussed, the coherent radiation is concentrated near the forward and backward scattering directions. In the forward direction, only a narrow frequency band at $\omega \approx \omega_L$ contributes to the spectrum. All this is in clear correspondence with the structure of the single-particle spectrum in the forward direction; see Eq. (14) and Fig. 2(b). In the backward direction, the largest contribution comes from the fundamental harmonics ω_1; see Eq. (21).

The approximation equation (24) fails in two major cases. First, for $R, L \ll \lambda$ the coherent radiation is no longer narrowly concentrated in the forward or backward directions, so the single-particle radiation spectrum $d\mathcal{E}^{(1)}/d\omega d\Omega$ has to be found by a fair numerical evaluation of the integral in Eq. (3). Second, the single-particle estimate equation (19) for the backscattering spectrum fails for $\omega < \omega_1$; see Fig. 3. Since this is not vital for our consideration here, we will present a refined analytical calculation of the single-particle spectrum, which resolves this issue, in a forthcoming publication [54].

III. MOMENTUM LOSS OF A SINGLE PARTICLE AND A BUNCH OF PARTICLES

Now let us turn to RF acting on particles in a laser pulse. As a measure of RF we use the amount of momentum taken away

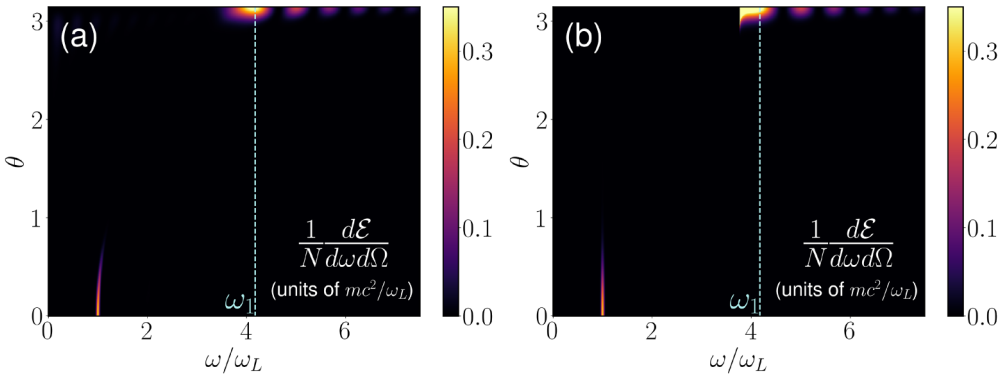


FIG. 4. Per-particle radiation spectrum of the Gaussian particle bunch [see Eq. (11)] of length $L = 0.1\lambda_L$, radius $R = 0.5\lambda_L$, $n = 0.01n_c$, and Lorentz factor $\gamma = 5$, colliding head on with a plane wave laser pulse with the Gaussian envelope equation (13), $a_0 = 5$, $\omega_L T = 15\pi$ (50 fs). (a) numerical evaluation of Eq. (6), (b) analytical estimate equation (24).

from the particles by radiation. We start with a known case of a single particle colliding with a pulsed plane electromagnetic wave. Then we consider a bunch of particles and express its momentum loss using the light-front momentum conservation in terms of contributions associated with forward and backward scattered coherent radiation.

A. Single particle

For a laser pulse taken as a plane wave solution of the Maxwell equations, such as, e.g., Eq. (13), the equation of motion (1) with the RF term in LL form can be solved exactly [9]. In particular, for the light component $p_- = \gamma mc - p_\parallel$ of energy momentum in a circularly polarized pulse, we have

$$p_-(\phi) = \frac{p_{-,0}}{1 + \mu \frac{p_{-,0}}{mc} \int_{-\infty}^{\phi} a^2(\phi')d\phi'}, \tag{25}$$

where $p_{-,0}$ is the initial value of p_-, $\boldsymbol{a}(\phi) = e\mathbf{E}(\phi)/m\omega_L c$ is the dimensionless field strength (note that we direct it along the electric field rather than along the vector potential), $\phi = \omega_L(t - x/c)$ is the phase, and μ was defined in Eq. (2). The exact expression for longitudinal momentum $p_\parallel$ is more involved, see Ref. [9], but in the relativistic case it can be roughly approximated simply by $p_\parallel \approx -p_-/2$.

Assume that RF is moderately strong, that is, $\Delta p_\parallel/p_0 \ll 1$, where $p_0 = p_\parallel(-\infty)$ is the initial value of $p_\parallel$. Then we immediately obtain

$$\Delta p_\parallel^{\mathrm{LL}} \approx \sqrt{2\pi}\mathcal{R}p_0, \tag{26}$$

where $\mathcal{R}$ was defined in Eq. (2). The factor $\sqrt{2\pi}$ comes due to the specific profile of the laser pulse envelope defined in Eq. (13). Note that up to this numerical factor Eq. (26) agrees with the condition equation (2) for the significance of RF.

The same result also follows from the calculation of the total energy radiated by the particle. Using the expression $d\mathcal{E}_{tot}^{(1)}/dt = -2r_e/3mc(dp_\mu/d\tau dp^\mu/d\tau)$ for the total radiated power [3], where p^μ is the 4-momentum of the particle and τ is its proper time, one obtains [55]

$$\mathcal{E}_{tot}^{(1)} = \mu c \int_{-\infty}^{\infty} \gamma a^2 p_- d\phi. \tag{27}$$

Assuming $\gamma \gg 1$, $\gamma \gg a_0$, and $\Delta p_\parallel \ll p_0$, the quantities γ and p_- remain almost constant and can be taken out of the integral. Furthermore, since an ultrarelativistic particle actually radiates almost along its propagation direction [26], we have $\Delta p_\parallel \approx \mathcal{E}_{\mathrm{tot}}^{(1)} \approx 2\mu mc^2\gamma^2 \int a^2(\phi)d\phi$, in agreement with Eq. (26).

B. Particle bunch

Next, consider the average momentum loss $\langle \Delta p_\parallel \rangle = \Delta P_\parallel/N$ of a particle in a bunch, where $\Delta P_\parallel$ is the total momentum loss of the whole bunch. Since it is *a priori* unknown how the RF force is modified to account for coherent radiation of the bunch, we calculate the momentum taken away by the radiation by means of the energy-momentum conservation using the coherent spectrum derived in Sec. II.

It is worth noting that we cannot calculate the energy loss of particles by the integration of the N-particle spectrum equation (6) over the solid angle and frequency. Indeed, the energy of the emitted radiation is taken not only from the particles but also from the laser pulse. On the other hand, the light cone momentum of the electromagnetic field P_-^{EM} changes from zero (for a plane wave laser pulse) to a positive value after scattering. Its increase is provided solely by the particles and $\Delta P_- = -\Delta P_-^{\mathrm{EM}}$, where P_- and P_-^{EM} denote the combination $P_- = \mathcal{E}/c - P_\parallel$ evaluated for the particle bunch and for the electromagnetic field, respectively. Assuming for simplicity that the particles are relativistic both before and after the collision with the laser pulse and therefore $p_\parallel = -p_-/2$, we get [56]

$$\langle \Delta p_\parallel \rangle \approx \frac{\pi}{cN} \int_0^\infty d\omega \int_0^\pi d\theta \frac{d\mathcal{E}}{d\omega d\Omega}(1 - \cos\theta)\sin\theta, \tag{28}$$

where, assuming the coherent radiation is dominant, we approximate the N-particle spectrum by Eq. (24). The structure of the approximated coherent radiation spectrum equation (24) suggests calculation of the forward and backward contributions to RF, corresponding to $\int_0^{\pi/2} d\theta$ and $\int_0^{\pi/2} d\theta$ in Eq. (28), separately.

Consider first the forward contribution. For a long pulse $\omega_L T \gg 1$, only a narrow band of frequencies close to the laser frequency ω_L contributes to the integral over ω, which thus casts to

$$\langle \Delta p_\parallel^f \rangle \approx mc \frac{\pi^2}{8\sqrt{2}} \frac{n}{n_c} \frac{a_0^2}{\gamma_0^2} \omega_L T \mathcal{G}, \tag{29}$$

where γ_0 is the initial γ factor of the particles in the bunch, n and $n_c = m\omega_L^2/4\pi e^2$ are the density of the bunch and the plasma critical density, respectively, and it is taken into account that $N = \pi^{3/2} nR^2 L/2$.

The remaining integral over θ takes the form

$$\mathcal{G} = \frac{\rho}{4\pi} \int_0^{\pi L/2\lambda_L} x e^{-\frac{x^2}{2} + \rho x^2 \frac{\lambda_L}{\pi L} - \rho x} dx, \tag{30}$$

where $x = (\pi L/\lambda_L)\sin^2(\theta/2)$, $\rho = 8\pi R^2/L\lambda_L$.

The geometric factor $\mathcal{G}$ includes the entire dependence of the forward contribution to RF on the sizes R and L of the bunch. To simplify Eq. (30) further, consider three cases:

(1) $R, L \ll \lambda_L$: the whole argument of the exponential in Eq. (30) is small; by replacing the exponential with unity we obtain

$$\mathcal{G}(R, L \ll \lambda_L) \approx \frac{\pi^2 R^2 L}{4\lambda_L^3}; \tag{31}$$

(2) $\rho \gg 1$ and $R \gtrsim \lambda_L$: in this case the effectively contributing $x \lesssim \rho^{-1} \ll 1$ and hence $\rho x^2 \lambda_L/(\pi L) \lesssim (\lambda_L/R)^2/(8\pi^2) \ll 1$. Therefore we can retain just the last term in the exponential in Eq. (30), thus arriving at

$$\mathcal{G}\left(\frac{R^2}{L\lambda_L} \gg 1, R \gtrsim \lambda_L\right) \approx \frac{L\lambda_L}{32\pi^2 R^2}; \tag{32}$$

(3) $\rho \ll 1$ and $L \gtrsim \lambda_L$: here the effectively contributing $x \lesssim 1$ and we can retain just the first term in the exponential to obtain

$$\mathcal{G}\left(\frac{R^2}{L\lambda_L} \ll 1, L \gtrsim \lambda_L\right) \approx \frac{2R^2}{L\lambda_L}. \tag{33}$$

In the case of Eq. (31) the whole bunch emits as a single macroparticle; hence the coherence of the scattering becomes maximal and the forward contribution to the momentum loss is naturally proportional to the number of particles in the bunch $N \sim nR^2 L$. Note, however, that in this case the radiation angular distribution is no longer narrow as assumed and hence the overall accuracy of Eq. (29) is poor.

If either $R \gtrsim \lambda_L$ or $L \gtrsim \lambda_L$, then the interference of radiation of all particles is constructive inside a cone with an opening angle $\delta\theta \lesssim 1$ and destructive elsewhere, implying that the radiation is coherent only inside this narrow cone. The value of $\delta\theta$ can be identified by demanding the coherence factor equation (11) essentially nonvanishing for $\omega \sim \omega_L$; that is, $\delta\theta \sim \lambda_L/R$ for $R^2/L\lambda_L \gg 1$ and $\delta\theta \sim \sqrt{\lambda_L/L}$ for $R^2/L\lambda_L \ll 1$. Since $\langle \Delta p_\parallel \rangle \sim \delta\theta^4$ for $\delta\theta \lesssim 1$, see Eq. (28), this way we deduce Eqs. (32) and (33) up to constant numerical factors directly from Eq. (31).

From Eqs. (32) and (33) it follows that the geometric factor $\mathcal{G}$ of a large bunch (either $R \gtrsim \lambda_L$ or $L \gtrsim \lambda_L$) has a maximum at a certain value of the parameter $\rho \sim R^2/L\lambda_L$; see Fig. 5. Let us estimate it for a thick bunch with $L \gtrsim \lambda_L$. First, observe that for $\rho \gg 1$ the geometric factor is suppressed as $\mathcal{G} \propto \rho^{-1} \ll 1$. If $\rho \lesssim 1$, then the second term in the exponential in Eq. (30) can be neglected, as only $x \lesssim 1$ effectively contribute to the integral due to the first term therein. Therefore,

$$\mathcal{G} \approx \frac{\rho}{4\pi}\left[1 - \sqrt{\frac{\pi}{2}}\rho e^{\frac{\rho^2}{2}} \mathrm{erfc}\left(\frac{\rho}{\sqrt{2}}\right)\right], \tag{34}$$

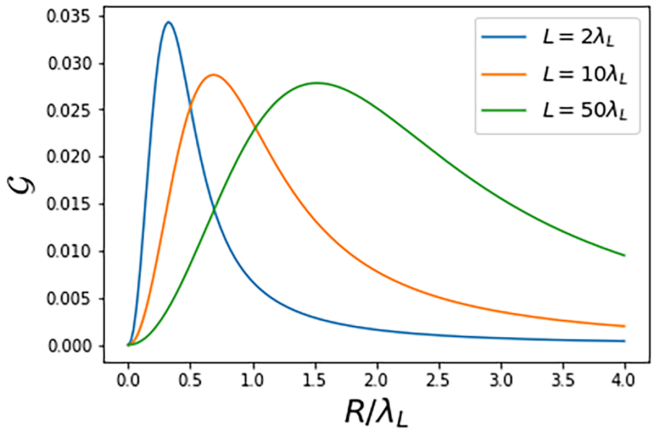


FIG. 5. Geometric factor $\mathcal{G}$, Eq. (30), vs bunch width R for three values of the bunch thickness L.

where $\mathrm{erfc}(z) = 1 - \mathrm{erf}(z)$ is the complementary error function. The numerical maximization of Eq. (34) provides

$$\mathcal{G}^m \approx 0.03 \quad \text{at} \quad \frac{R^2}{L\lambda_L} \approx 0.05. \tag{35}$$

Direct evaluation of the integral equation (30) confirms the estimate of its maximum and the optimal shape $R \sim \sqrt{L\lambda_L}$; see Fig. 5.

The geometric factor equation (30) can be expressed in a closed form as

$$\mathcal{G} = \frac{\sqrt{A}B(e^{A^2} - e^{B^2} + \sqrt{\pi}B[\mathrm{erfi}(B) - \mathrm{erfi}(A)])}{2\sqrt{2}\pi e^{B^2}\sqrt{B - A}}, \tag{36}$$

where $A = \pi L^2/[2\lambda_L\sqrt{2(16R^2 - L^2)}]$ and $B = 4\sqrt{2}\pi R^2/(\lambda_L\sqrt{16R^2 - L^2})$ and $\mathrm{erfi}(z)$ is the imaginary error function.

Now let us turn to the backward contribution $\langle \Delta p_\parallel^b \rangle$. Substituting Eqs. (6), (11), and (19) into Eq. (28) and replacing $\cos\theta \to -1$, $\sin(\theta/2) \to 1$, we obtain

$$\langle \Delta p_\parallel^b \rangle \approx mc\frac{\sqrt{\pi}}{16}\frac{n}{n_c}\frac{\omega_L^4 R^2 LT}{c^3}\mathcal{I},$$
$$\mathcal{I} = \int e^{-\frac{\omega^2}{2c^2}\left(\frac{L^2}{4} + R^2\sin^2\theta\right)}\frac{1 + \sin\eta}{\nu}\frac{\omega d\omega}{\omega_L^2}\sin\theta d\theta, \tag{37}$$

where η and ν are defined in Eq. (20). Here the integration over frequency effectively starts from the vicinity of the position ω_1 of the first peak in the single-particle radiation spectrum as defined in Eq. (21) (see Fig. 3 and its discussion). On the opposite side, integration formally extends to infinity, but Eq. (3) in use is valid only for $\omega < \omega_*$. Nevertheless, under quite a weak condition, $\omega_* L/c \gg 1$, the integrand falls out exponentially already within the applicability range, so that we can still use Eq. (3) integrating up to infinity.

As repeatedly emphasized, for our analytical approach we assume that the radiation is emitted in a narrow angle; i.e., a short angular range contributes to the integral. As suggested by Eq. (37), this is indeed the case, if $\omega_1 R/c \gg 1$. Then, expanding $\sin\theta \approx \pi - \theta$, integrating over θ, and using

$\omega \approx \omega_1 e^{\nu^2/2}$ (which is valid for $\omega \ll \omega_*$), we get

$$\mathcal{I} \approx \frac{c^2}{\omega_L^2 R^2} \int_0^\infty e^{-\frac{\omega_1^2 L^2 e^{\nu^2}}{8c^2}} (1+\sin\eta) d\nu. \tag{38}$$

The resulting integral in Eq. (38) can be approximated analytically assuming the bunch is thick enough. In this case the effectively contributing ν are small $\nu \lesssim c/(\omega_1 L)$, so that we can expand $e^{\nu^2} \approx 1+\nu^2$ and $\eta \approx \omega_L T \nu^3/3$. Finally, expanding also $\sin\eta$ and assuming $\omega_1 L/c \gtrsim 1$ and $\omega_1 L/c \gtrsim (\omega_L T)^{1/3}$, we obtain

$$\langle \Delta p_\parallel^b \rangle \approx mc \frac{\pi \omega_L T}{32\sqrt{2}} \frac{a_0^2}{\gamma_0^2} \frac{n}{n_c} e^{-\frac{\pi^2 L^2}{2\lambda_1^2}}, \tag{39}$$

where $\lambda_1 \approx \frac{\lambda_L(1+a_0^2)}{4\gamma_0^2}$ is the wavelength of the fundamental harmonic of the backward radiation.

Let us represent the total average momentum loss due to coherently enhanced RF in the form

$$\langle \Delta p_\parallel \rangle \approx \langle \Delta p_\parallel^f \rangle (1+\upsilon), \quad \upsilon = \frac{\langle \Delta p_\parallel^b \rangle}{\langle \Delta p_\parallel^f \rangle} = \frac{e^{-\frac{\pi^2 L^2}{2\lambda_1^2}}}{4\pi \mathcal{G}}, \tag{40}$$

where $\langle \Delta p_\parallel^f \rangle$ is defined in Eq. (29). For a thick bunch, $L \gg \lambda_1$, the backward radiation is suppressed, $\upsilon \ll 1$, and only forward radiation contributes to RF.

Being proportional to the particle density, the effect is essential for a dense bunch with $n \sim n_c$ (for an optical laser $n_c \sim 10^{21}\,\mathrm{cm}^{-3}$) or a few orders of magnitude lower; see the companion Letter, Ref. [44]. Quasimonoenergetic bunches with $n \sim 10^{18} - 10^{19}\,\mathrm{cm}^{-3}$ have been already obtained experimentally [57–59] and some ways to generate bunches with $n \sim 10^{21}\,\mathrm{cm}^{-3}$ and even higher have been discussed in, e.g., Refs. [60–65].

Three-dimensional particle-in-cell simulations reported in the companion Letter (Ref. [44]) demonstrate high accuracy of the approximation equation (40) for $\langle \Delta p_\parallel \rangle \ll p_0$. If this inequality is violated, this means that RF is so strong that it significantly perturbs the particle motion. In such a case the expressions for the single-particle radiation spectra equations (14) and (19) obtained by neglecting the effect of RF on the particle trajectories are no longer valid, at least quantitatively.

IV. DISCUSSION

In order to compare the effect of coherently enhanced RF equation (40) with the known single-particle result equation (26), let us write their ratio as

$$\frac{\langle \Delta p_\parallel \rangle}{\Delta p_\parallel^{LL}} \approx \frac{\pi^{3/2}}{16} \frac{n}{n_c} \frac{(1+\upsilon)\mathcal{G}}{\mu \gamma_0^4}. \tag{41}$$

The denominator contains μ, which for an optical or infrared laser is small, $\mu \sim 10^{-8} - 10^{-9}$. As a consequence, RF can be coherently enhanced at low frequencies by orders of magnitude [35] by using mildly relativistic particle bunches. This is clearly seen by comparing the single-particle radiation spectrum in Fig. 2(b), which corresponds to the per-particle incoherent contribution, to the actual total radiation spectrum in Fig. 4.

On the other hand, due to the presence of the Lorentz factor in the denominator of Eq. (41), for ultrarelativistic bunches the incoherent contribution to RF always overcomes the coherent one. This is explained by the fact that for $a_0 \gtrsim 1$ and $\gamma \gg 1$ the incoherent single-particle spectrum is much broader, extending up to frequencies $\omega \lesssim a_0(a_0^2+\gamma_0^2)\omega_L$; see Fig. 2(b) and Refs. [3,26,66]. Further comparison of the properties of ordinary and coherently enhanced RF can be found in the companion Letter [44].

Next let us study the sensitivity of our results with respect to the simplifications in use, such as the assumed circular polarization (CP) equation (13) of the laser pulse and the specific (Gaussian) density profile of the particle bunch.

For an arbitrary elliptical polarization,

$$\mathbf{A} = \frac{mca_0}{e} \sqrt{\frac{2}{1+\varepsilon^2}} e^{-\phi^2/(\omega_L T)^2} \{0, \cos\phi, \varepsilon \sin\phi\}, \tag{42}$$

the single-particle spectrum in the forward direction (12) coincides with the CP result equation (14), i.e., is independent of polarization ε. As for the backward spectrum, one can demonstrate [54] that for $a_0 \gg 1$ in the vicinity of the first harmonic $\omega \sim \omega_1$ that mostly contributes to the coherent radiation,

$$\left.\frac{d\mathcal{E}^{(1)}}{d\omega d\Omega}\right|_{\theta=\pi}^{\varepsilon} \approx \mathcal{R}_\varepsilon \left.\frac{d\mathcal{E}^{(1)}}{d\omega d\Omega}\right|_{\theta=\pi}^{\varepsilon=1}, \quad \mathcal{R}_\varepsilon = 1 - \frac{1}{2}\left(\frac{1-\varepsilon^2}{1+\varepsilon^2}\right)^2, \tag{43}$$

where $d\mathcal{E}^{(1)}/d\omega d\Omega|_{\theta=\pi}^{\varepsilon=1}$ is the single-particle backward spectrum for CP; see Eq. (19).

Thus, since the coherence factor α is obviously independent of ε, the effect of polarization on the coherently enhanced RF is given by

$$\frac{\langle \Delta p_\parallel^\varepsilon \rangle}{\langle \Delta p_\parallel^{\mathrm{CP}} \rangle} \approx \frac{1+\mathcal{R}_\varepsilon \upsilon}{1+\upsilon}, \tag{44}$$

where $\langle \Delta p_\parallel^\varepsilon \rangle$ is the momentum loss in an elliptically polarized pulse, $\langle \Delta p_\parallel^{\mathrm{CP}} \rangle$ is the CP result equation (40), and the ratio between the backward and forward contributions υ in the CP case was defined in Eq. (40).

According to Eq. (44), for a thick bunch such that the backward contribution is negligible, $\upsilon \ll 1$ and RF is independent of polarization. In the opposite case $\upsilon \gg 1$ the effect for the linear polarization $\varepsilon = 0$ is approximately twice as weak than for CP. This is in agreement with the results of PIC simulations shown in Fig. 6; see the companion Letter [44] for the description of the numerical approach.

To check the dependence on the initial density profile of the bunch, we consider an alternative bunch model of a uniform cylinder of length L and radius R. The analytical calculation follows the same lines as for the Gaussian density distribution equation (11) in Secs. II and III; see the Appendix for details. We found the results for these two density distributions quite similar, meaning that the effect is robust with respect to the particular shape of the bunch, which is hard to control in experiments anyway.

In particular, the forward contribution to RF can be represented by the same equation (29) as in the Gaussian case, but

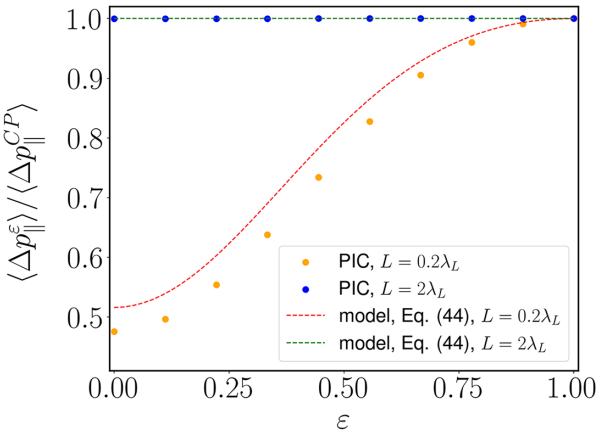


FIG. 6. Dependence of the momentum loss on laser polarization. Parameters: $a_0 = \gamma_0 = 5$, $T \approx 17$ fs, $R = 2\lambda_L$, $n = 0.1 n_c$.

with a different geometric factor,

$$\mathcal{G}_u = \pi^{-3/2} \int_0^{\frac{\pi L}{2\lambda_L}} \frac{J_1^2\left(\sqrt{2\rho x\left(1 - \frac{\lambda_L}{\pi L} x\right)}\right) \sin^2 x dx}{x^2\left(1 - \frac{\lambda_L}{\pi L} x\right)}, \qquad (45)$$

where ρ and x are the same as defined below Eq. (30). It is about twice as large as the Gaussian one but otherwise behaves similarly, see Fig. 7, in particular, reaching its maximum at $R^2/L\lambda_L \approx 0.05$, as in Eq. (35).

V. SUMMARY

We have studied radiation losses of a dense particle bunch colliding head on with a laser pulse. We developed an analytical model, which describes the average momentum losses of particles in the bunch in dependence on various laser and bunch parameters, such as laser pulse intensity, duration, and polarization; and bunch size, density, and initial energy. The model unfolds the conditions for a strong coherent enhancement of radiation in the forward and backward directions at low frequencies, thus also for enhancement of radiation friction. It is shown that the results are marginally sensitive to laser polarization and density distribution of the particle bunch. Numerical simulations supporting our analytical findings (including the effect of the here neglected momentum spread of the particles in the bunch) and further discussion of physical origins of the coherently enhanced radiation friction, its distinction from the ordinary noncoherent radiation friction, and the prospects for experimental observation can be found in the companion Letter, Ref. [44].

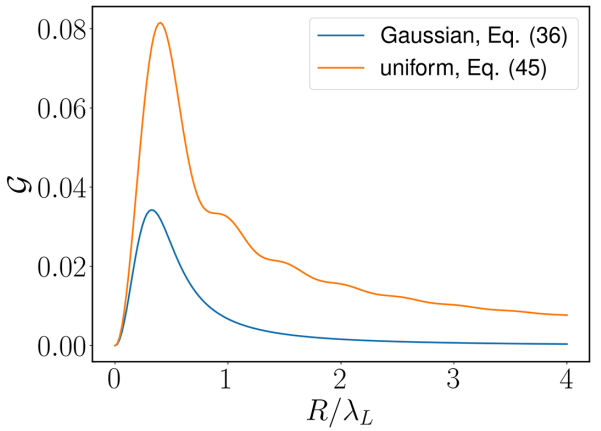


FIG. 7. Geometric factors for Gaussian and uniform distributions of the bunch density.

ACKNOWLEDGMENTS

The authors are grateful to A. D. Piazza, M. Tamburini, M. Grech, C. Riconda, S. Rykovanov, I. Kostyukov, V. Tikhonchuk, M. Stack Formanek, and P. Valenta for valuable discussions. E.G.G., J.C., O.K., and S.W. were supported by Czech Science Foundation Project No. 24-14395L in the frame of the NSF–GACR partnership. A.M.F. was supported by the Russian Science Foundation (Grant No. 25-12-00336). Th.B. was supported by the ELI Beamlines internship program (2025). The numerical simulations were performed using the code SMILEI and the resources of the ELI ERIC SUNRISE cluster.

DATA AVAILABILITY

The data that support the findings of this article are not publicly available upon publication because it is not technically feasible and/or the cost of preparing, depositing, and hosting the data would be prohibitive within the terms of this research project. The data are available from the authors upon reasonable request.

APPENDIX: RADIATION AND RADIATION FRICTION OF A UNIFORMLY DISTRIBUTED PARTICLE BUNCH

To test the robustness of our results, consider a cylindrical particle bunch of length L and radius R with a uniform density distribution $n(x, \mathbf{r}_\perp) = n_0\theta(x)\theta(L - x)\theta(R - r_\perp)$, where $\theta(x)$ is the Heaviside step function. Then for the coherence factor $\alpha = |\langle e^{i\Phi}\rangle|^2$ we obtain [67]

$$\alpha = \frac{16c^4 J_1^2\left(\frac{\omega R}{c}\sin\theta\right)\sin^2\left(\frac{\omega L}{2c}\sin^2\frac{\theta}{2}\right)}{R^2L^2\omega^4\sin^2\theta\sin^4\frac{\theta}{2}}, \qquad (A1)$$

where $J_1(x)$ is the Bessel function and the initial phases Φ_j are defined as in Eq. (8).

Let us calculate the momentum transfer Eq. (28) for a uniform bunch, again considering the forward and backward contributions separately. While evaluating the backward contribution $\langle \Delta p_\parallel^b \rangle$, we assume that the bunch size is larger than the wavelength of the lowest backward scattered harmonic and that the pulse is longer than at least a few laser periods,

$$\omega_1 R/c \gtrsim 1, \quad \omega_1 L/c \gtrsim 1, \quad \omega_L T \gg 1. \qquad (A2)$$

Note that this does not necessarily imply that the bunch is larger than the laser wavelength, as in our setup $\omega_1 > \omega_L$ for $\gamma_0 > a_0$.

Under the conditions (A2) the backward radiation sharply peaks around $\theta = \pi$ [35], and, as before, we substitute into Eq. (28) $\sin(\theta/2) \to 1$, $\cos\theta \to -1$ and use $d\mathcal{E}^{(1)}/d\omega d\Omega$ from Eq. (19). Furthermore, in the integral over frequency we replace the lower limit with ω_1 where starts the single-particle

spectrum, and the upper limit with infinity due to a fast fallout of $\alpha \propto \omega^{-5}$ at high frequencies; see Eq. (A1).

With all the above adjustments we obtain

$$\langle \Delta p_\parallel^b \rangle \approx \frac{4Ne^2c^3T}{R^2L^2} \int_{\omega_1}^{\infty} \frac{1+\sin\eta}{\omega^3\nu} \sin^2 \frac{\omega L}{2c} d\omega, \tag{A3}$$

in particular, by taking into account that

$$\int_{\pi/2}^{\pi} \frac{J_1^2\left(\frac{\omega R}{c}\sin\theta\right)}{\sin\theta} d\theta \approx \frac{1}{2}, \tag{A4}$$

for $\omega R/c \gtrsim 1$, when the angular range $\pi - c/\omega R \lesssim \theta < \pi$ effectively contributing to the integral in Eq. (A4) is narrow [68].

To evaluate the remaining integral over frequency, we change the integration variable to ν and observe that, since the largest contribution comes from the lower integration limit, we can approximate $\nu \approx \sqrt{2\ln(\omega/\xi^2\omega_L)}$ for $a_0 \gg 1$, thus obtaining

$$\langle \Delta p_\parallel^b \rangle \approx \frac{4Ne^2c^3T}{\omega_L^2R^2L^2\xi^4} \int_{\sqrt{2\delta}}^{\infty} (1+\sin\eta) e^{-\nu^2} \sin^2\Lambda d\nu, \tag{A5}$$

where $\Lambda = \xi^2\omega_L L e^{\nu^2/2}/2c$ and δ is defined in Eq. (21).

In the remaining integral, we assume that $\xi^2\omega_L L/c \gg 1$ and average the integrand over the oscillations of $\sin^2\Lambda$ by replacing the latter with $1/2$. To evaluate the term with $\sin\eta$ we observe that the main contribution to the integral comes from frequencies $\omega \ll \omega_*$ and Taylor expand $\eta \approx \omega_L T\nu^3/3$. Furthermore, assuming $\omega_L T \gg 1$, we see that $\sin(\omega_L T\nu^3/3)$ undergoes rapid oscillations suppressing the integral unless $\nu \ll 1$; hence in this term we approximate $e^{-\nu^2} \approx 1$. The other term is evaluated directly. Thus we arrive at

$$\langle \Delta p_\parallel^b \rangle \approx \frac{mca_0^4}{128\sqrt{\pi}\gamma_0^4} \frac{n}{n_c} \frac{\lambda_L}{L} \mathcal{T}(\omega_L T),$$
$$\mathcal{T}(t) = t\left\{ \mathrm{erfc}\left[\left(\frac{3\pi}{2t}\right)^{1/3} \right] + \beta t^{-1/3} \right\}, \tag{A6}$$

where $\beta = (2/3^{2/3}\sqrt{\pi}) \int_{\pi/2}^{\infty} \sin\eta\, \eta^{-2/3} d\eta \approx 0.097$ and we took into account that $N = \pi n R^2 L$. Note that for $\omega_L T \to \infty$ we have $\mathcal{T}(\omega_L T) \to \omega_L T$. However, in numerical simulations below we take $\omega_L T = 5\pi$ (as corresponding to $T \approx 17$ fs), for which $\mathcal{T}(\omega_L T) \approx 0.38$. For this reason in the sequel we avoid further simplifications of the function $\mathcal{T}(\omega_L T)$.

To check the validity of the approximations resulted in the analytical result equation (A6) we benchmark it against the numerical evaluation of Eq. (A3). Figure 8 demonstrates that Eq. (A6) is fairly accurate for $L \gtrsim \lambda_L$ and $\omega_L T = 5\pi$ as used in numerical simulations below. The oscillations in Fig. 8 clearly appear due to the actual oscillations of the factor $\sin^2(\omega L/2c)$ in Eq. (A3) and a small discrepancy in the mean values arises due to our approximation $e^{-\nu^2} \approx 1$ in the evaluation of the term that involves $\sin\eta$.

For the forward contribution $\langle \Delta p_\parallel^f \rangle$ to the momentum loss, we obtain an expression similar to the Gaussian case (29), but with a different geometric factor equation (45). Unlike the Gaussian case, here the integral representing the geometric factor $\mathcal{G}_u$ cannot be evaluated exactly. However, it can still be

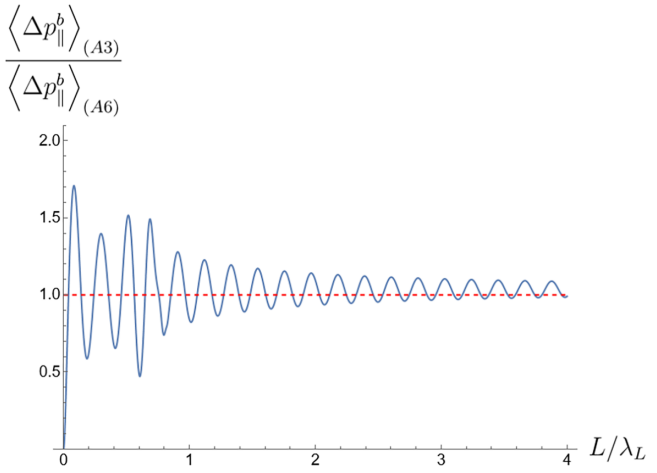


FIG. 8. Ratio of the backward contribution to the momentum loss evaluated numerically via Eq. (A3) and analytically via Eq. (A6) for $\omega_L T = 5\pi$.

approximated analytically under further assumptions on the bunch sizes R and L:

$$\mathcal{G}_u(L \ll \lambda_L, R \ll \lambda_L) = \frac{\pi^{3/2}}{2} \frac{R^2 L}{\lambda_L^3}, \tag{A7a}$$

$$\mathcal{G}_u(L \ll \lambda_L, R \gg \lambda_L) = \frac{1}{2\pi^{5/2}} \frac{L}{R}, \tag{A7b}$$

$$\mathcal{G}_u\left(L \gtrsim \lambda_L, \frac{R^2}{L\lambda_L} \gg 1\right) = \frac{1}{3\pi^{5/2}} \frac{\sqrt{L\lambda_L}}{R}, \tag{A7c}$$

$$\mathcal{G}_u\left(L \gtrsim \lambda_L, \frac{R^2}{L\lambda_L} \ll 1\right) = \frac{2}{\sqrt{\pi}} \frac{R^2}{\lambda_L L}\left(C + \ln\frac{\pi L}{\lambda_L}\right), \tag{A7d}$$

where C is the Euler constant.

For a thin bunch $L \ll \lambda_L$ we pass from Eq. (45) to Eqs. (A7a) and (A7b) by approximating $\sin^2 x/x^2 \approx 1$ and expanding the Bessel function for either small (if $R \ll \lambda_L$) or large (if $R \gg \lambda_L$) argument, respectively. Again, similar to the Gaussian case, if both sizes of the bunch are much smaller than the laser wavelength, then $\langle \Delta p_\parallel^f \rangle$ is proportional to N and independent of the shape of the bunch, simply meaning that in this case all the particles in the bunch emit coherently at $\omega \sim \omega_L$.

In the opposite case, $L \gtrsim \lambda_L$, the major contribution to the integral in Eq. (45) comes from $x \lesssim 1$ due to the factor $\sin^2 x/x^2$. Physically, this restricts the width of the radiation angular distribution [35]. Hence we Taylor expand in powers of $\lambda_L/\pi L < 1$ and also expand the Bessel function for either large or small argument with respect to ρ, thus arriving at Eq. (A7c) or Eq. (A7d). Figure 9 demonstrates the accuracy of the resulting analytical approximations (A7). Note that for $L \ll \lambda_L$ the geometric factor $\mathcal{G}_u$ attains its maximum at $R \sim \lambda_L/3$ independently of the value of L (Fig. 9, top), while for $L \gtrsim \lambda_L$ (Fig. 9, bottom) the position of the maximum increases with L in agreement with Eq. (35).

Figure 10 illustrates the dependence of the coherent RF on a transverse size R of a bunch with a uniform initial density as extracted from three-dimensional (3D) PIC simulations

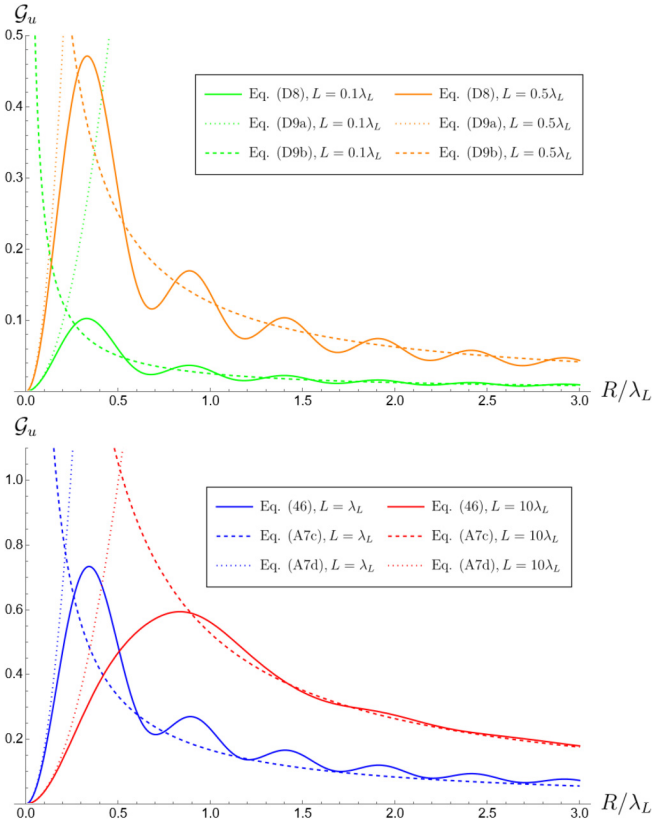


FIG. 9. Comparison of the analytical approximations (A7) for the geometric factor $\mathcal{G}$ (dotted and dashed lines) vs direct numerical evaluation of Eq. (45) (solid lines) for several bunch lengths L. Green, orange, blue, and red correspond to $L/\lambda_L = 0.1$, 0.5, 1, and 10, respectively.

(the numerical approach is described in the companion Letter [44]). In accordance with Eq. (A7) one can clearly see a crossover between the small and large R asymptotics where RF is maximized. Its position at the intersection of the green and purple curves matches the condition (35). As we have already noted, the numerical value 0.05 of the constant in Eq. (35) turns out to be close for the uniformly and Gaussian distributed bunches. It is worth stressing that whereas the backward contribution can be actually neglected for small R, taking it into account for large R considerably improves the accuracy of the model.

Finally, let us compare the results for the uniform and Gaussian density distributions. Whereas in the Gaussian case for $L > \lambda_1$, where $\lambda_1 \approx \hat{\lambda}$ is the wavelength of the first harmonic in the backward radiation spectrum, the backward

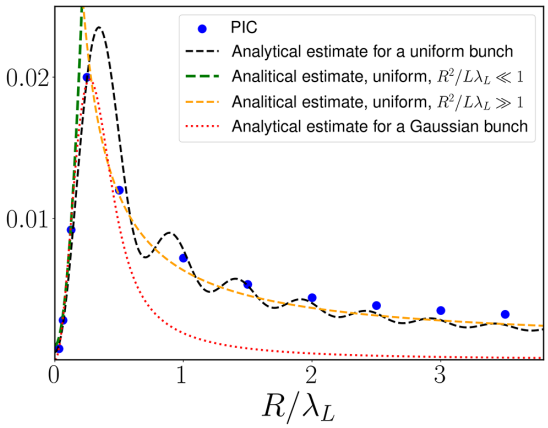


FIG. 10. Normalized particle deceleration $\langle \Delta p_\parallel \rangle / p_0$ vs bunch width R for a cylindrical bunch of uniform density distribution. Blue dots are extracted from 3D PIC simulations. Dashed curves correspond to the sum of Eq. (29) + Eq. (A6) with $\mathcal{G}$ from Eqs. (45) (black), (A7c) (orange), and (A7d) (green). Red dotted curve corresponds to the Gaussian estimate (29) with $\mathcal{G}$ from Eq. (36) multiplied by a scale factor of 2. Other parameters are $a_0 = 5$, $\omega_L T = 5\pi$, $n = 0.1 n_c$, and $L = \lambda_L$.

contribution (39) falls out exponentially. For a uniform distribution it falls out as $1/L$; see Eq. (A6). In addition, in contrast to the former case, its dependence on L actually becomes oscillatory. The origin of these oscillations can be understood as follows. Backward radiation from particles in a slice of thickness $\lambda_1/2$ interferes constructively, but destructively from such adjacent slices. Therefore, if the thickness of the whole bunch $L = m\lambda_1$, where m is an integer, then the backward radiation vanishes, while it is maximal for $L = (m + 1/2)\lambda_1$. These oscillations correspond to the factors $\sin^2[\omega L \sin^2(\theta/2)/2c]$ in Eq. (A1) and $\sin^2(\omega L/2c)$ in Eq. (A3); for simplicity we averaged them out in our final expression (A6).

For a thick ($L \gtrsim \lambda_L$) bunch and $R^2/L\lambda_L \lesssim 1$ the forward contribution dominates over the backward one for both uniform and Gaussian density distributions. In this regime the scaling of RF with laser and bunch parameters for both distributions is in fact quite similar; cf. Eqs. (33) and (A7d). Figure 10 demonstrates that for $R \lesssim \sqrt{L\lambda_L}$ the scaling for a Gaussian bunch almost perfectly matches the simulation results for a uniform bunch up to a constant scaling factor. As for $R \gg \sqrt{L\lambda_L}$, the forward contribution $\langle \Delta p_\parallel^f \rangle$ decreases as R^{-2} in the Gaussian case and as R^{-1} in the uniform case, so that at some point the backward contribution can become dominant in both cases.

[1] P. A. M. Dirac, Classical theory of radiating electrons, Proc. A **167**, 148 (1938).
[2] L. D. Landau and I. M. Lifshitz, *The Classical Theory of Fields*, Course of Theoretical Physics, Vol. 2 (Pergamon Press, London, 1988).
[3] J. D. Jackson, *Classical Electrodynamics* (John Wiley & Sons, New York, 2021).
[4] J. M. Cole, K. T. Behm, E. Gerstmayr, T. G. Blackburn, J. C. Wood, C. D. Baird, M. J. Duff, C. Harvey, A. Ilderton, A. S. Joglekar, *et al.*, Experimental evidence of radiation reaction in the collision of a high-intensity laser pulse with a laser-wakefield accelerated electron beam, Phys. Rev. X **8**, 011020 (2018).
[5] K. Poder, M. Tamburini, G. Sarri, A. Di Piazza, S. Kuschel, C. D. Baird, K. Behm, S. Bohlen, J. M. Cole, D. J. Corvan, *et al.*, Experimental signatures of the quantum nature of radiation reaction in the field of an ultraintense laser, Phys. Rev. X **8**, 031004 (2018).

[6] E. E. Los, E. Gerstmayr, C. Arran, M. J. Streeter, C. Colgan, C. C. Cobo, B. Kettle, T. G. Blackburn, N. Bourgeois, L. Calvin, *et al.*, Observation of quantum effects on radiation reaction in strong fields, Nat. Commun. **17**, 1157 (2026).

[7] B. Voronin and A. Kolomenskii, The pressure of an intense plane wave on a free charge and on a charge in a magnetic field, Sov. Phys. JETP **20**, 1027 (1965).

[8] Y. B. Zel'Dovich, Interaction of free electrons with electromagnetic radiation, Sov. Phys. Usp. **18**, 79 (1975).

[9] A. D. Piazza, Exact solution of the Landau–Lifshitz equation in a plane wave, Lett. Math. Phys. **83**, 305 (2008).

[10] M. Tamburini, F. Pegoraro, A. Di Piazza, C. H. Keitel, and A. Macchi, Radiation reaction effects on radiation pressure acceleration, New J. Phys. **12**, 123005 (2010).

[11] M. Tamburini, F. Pegoraro, A. Di Piazza, C. H. Keitel, T. V. Liseykina, and A. Macchi, Radiation reaction effects on electron nonlinear dynamics and ion acceleration in laser–solid interaction, Nucl. Instrum. Methods Phys. Res. Sect. A **653**, 181 (2011).

[12] M. Tamburini, T. V. Liseykina, F. Pegoraro, and A. Macchi, Radiation-pressure-dominant acceleration: Polarization and radiation reaction effects and energy increase in three-dimensional simulations, Phys. Rev. E **85**, 016407 (2012).

[13] M. Chen, A. Pukhov, T.-P. Yu, and Z.-M. Sheng, Radiation reaction effects on ion acceleration in laser foil interaction, Plasma Phys. Controlled Fusion **53**, 014004 (2011).

[14] R. Capdessus and P. McKenna, Influence of radiation reaction force on ultraintense laser-driven ion acceleration, Phys. Rev. E **91**, 053105 (2015).

[15] E. Gelfer, A. Fedotov, and S. Weber, Radiation induced acceleration of ions in a laser irradiated transparent foil, New J. Phys. **23**, 095002 (2021).

[16] E. Gelfer, N. Elkina, and A. Fedotov, Unexpected impact of radiation friction: Enhancing production of longitudinal plasma waves, Sci. Rep. **8**, 6478 (2018).

[17] E. Gelfer, A. Fedotov, and S. Weber, Theory and simulations of radiation friction induced enhancement of laser-driven longitudinal fields, Plasma Phys. Controlled Fusion **60**, 064005 (2018).

[18] T. Liseykina, S. Popruzhenko, and A. Macchi, Inverse Faraday effect driven by radiation friction, New J. Phys. **18**, 072001 (2016).

[19] S. Popruzhenko, T. Liseykina, and A. Macchi, Efficiency of radiation friction losses in laser-driven 'hole boring' of dense targets, New J. Phys. **21**, 033009 (2019).

[20] J. Koga, T. Z. Esirkepov, and S. V. Bulanov, Nonlinear Thomson scattering in the strong radiation damping regime, Phys. Plasmas **12**, 093106 (2005).

[21] A. Di Piazza, K. Z. Hatsagortsyan, and C. H. Keitel, Quantum radiation reaction effects in multiphoton Compton scattering, Phys. Rev. Lett. **105**, 220403 (2010).

[22] N. Neitz and A. Di Piazza, Stochasticity effects in quantum radiation reaction, Phys. Rev. Lett. **111**, 054802 (2013).

[23] A. G. R. Thomas, C. P. Ridgers, S. S. Bulanov, B. J. Griffin, and S. P. D. Mangles, Strong radiation-damping effects in a gamma-ray source generated by the interaction of a high-intensity laser with a wakefield-accelerated electron beam, Phys. Rev. X **2**, 041004 (2012).

[24] F. Sauter, Über das Verhalten eines Elektrons im homogenen elektrischen Feld nach der relativistischen Theorie Diracs, Z. Phys. **69**, 742 (1931).

[25] J. Schwinger, On gauge invariance and vacuum polarization, Phys. Rev. **82**, 664 (1951).

[26] V. I. Ritus, Quantum effects of the interaction of elementary particles with an intense electromagnetic field, J. Russ. Laser Res. **6**, 497 (1985).

[27] A. Di Piazza, C. Müller, K. Z. Hatsagortsyan, and C. H. Keitel, Extremely high-intensity laser interactions with fundamental quantum systems, Rev. Mod. Phys. **84**, 1177 (2012).

[28] C. J. Eliezer, On the classical theory of particles, Proc. A **194**, 543 (1948).

[29] G. Ford and R. O'Connell, Radiation reaction in electrodynamics and the elimination of runaway solutions, Phys. Lett. A **157**, 217 (1991).

[30] D. A. Burton and A. Noble, Aspects of electromagnetic radiation reaction in strong fields, Contemp. Phys. **55**, 110 (2014).

[31] A. Gonoskov, T. G. Blackburn, M. Marklund, and S. S. Bulanov, Charged particle motion and radiation in strong electromagnetic fields, Rev. Mod. Phys. **94**, 045001 (2022).

[32] A. Fedotov, A. Ilderton, F. Karbstein, B. King, D. Seipt, H. Taya, and G. Torgrimsson, Advances in QED with intense background fields, Phys. Rep. **1010**, 1 (2023).

[33] F. V. Hartemann, Stochastic electron gas theory of coherence in laser-driven synchrotron radiation, Phys. Rev. E **61**, 972 (2000).

[34] A. Gonoskov, S. Bastrakov, E. Efimenko, A. Ilderton, M. Marklund, I. Meyerov, A. Muraviev, A. Sergeev, I. Surmin, and E. Wallin, Extended particle-in-cell schemes for physics in ultrastrong laser fields: Review and developments, Phys. Rev. E **92**, 023305 (2015).

[35] E. G. Gelfer, A. M. Fedotov, O. Klimo, and S. Weber, Coherent radiation of an electron bunch colliding with an intense laser pulse, Phys. Rev. Res. **6**, L032013 (2024).

[36] E. G. Gelfer, A. M. Fedotov, O. Klimo, and S. Weber, Collective coherent emission of electrons in strong laser fields and perspective for hard x-ray lasers, Matter Radiat. Extremes **9**, 024201 (2024).

[37] J. Schwinger, On radiation by electrons in a betatron, preprint LBNL–39088, July 1996, in *A Quantum Legacy: Seminal Papers of Julian Schwinger* (World Scientific, Singapore, 2000).

[38] F. C. Michel, Intense coherent submillimeter radiation in electron storage rings, Phys. Rev. Lett. **48**, 580 (1982).

[39] C. J. Hirschmugl, M. Sagurton, and G. P. Williams, Multiparticle coherence calculations for synchrotron-radiation emission, Phys. Rev. A **44**, 1316 (1991).

[40] J. Vieira, M. Pardal, J. Mendonça, and R. Fonseca, Generalized superradiance for producing broadband coherent radiation with transversely modulated arbitrarily diluted bunches, Nat. Phys. **17**, 99 (2021).

[41] B. Malaca, M. Pardal, D. Ramsey, J. Pierce, K. Weichman, I. Andriyash, W. Mori, J. Palastro, R. Fonseca, and J. Vieira, Coherence and superradiance from a plasma-based quasiparticle accelerator, Nat. Photon. **18**, 39 (2024).

[42] M. J. Quin, A. Di Piazza, and M. Tamburini, Coherent frequency combs from electrons colliding with a laser pulse, Plasma Phys. Controlled Fusion **67**, 055008 (2025).

[43] M. J. Quin, A. Di Piazza, C. H. Keitel, and M. Tamburini, Effect of interparticle fields and radiation reaction on beam dynamics, Phys. Rev. Res. **7**, 023210 (2025).
[44] E. G. Gelfer, A. M. Fedotov, M. P. Malakhov, O. Klimo, and S. Weber, companion paper, Coherently enhanced radiation friction in laser-Plasma collisions, Phys. Rev. Lett. **137**, 095001 (2026).
[45] The role is investigated numerically in the companion Letter [44]; see also [42].
[46] L. I. Schiff, Production of particle energies beyond 200 MeV, Rev. Sci. Instrum. **17**, 6 (1946).
[47] A. G. R. Thomas, Algorithm for calculating spectral intensity due to charged particles in arbitrary motion, Phys. Rev. ST Accel. Beams **13**, 020702 (2010).
[48] M. Boca and V. Florescu, Nonlinear Compton scattering with a laser pulse, Phys. Rev. A **80**, 053403 (2009).
[49] D. Seipt and B. Kämpfer, Nonlinear Compton scattering of ultrashort intense laser pulses, Phys. Rev. A **83**, 022101 (2011).
[50] F. V. Hartemann, A. L. Troha, N. C. Luhmann, Jr., and Z. Toffano, Spectral analysis of the nonlinear relativistic Doppler shift in ultrahigh intensity Compton scattering, Phys. Rev. E **54**, 2956 (1996).
[51] D. Seipt and B. Kämpfer, Nonlinear Compton scattering of ultrahigh-intensity laser pulses, Laser Phys. **23**, 075301 (2013).
[52] V. Y. Kharin, D. Seipt, and S. G. Rykovanov, Temporal laser-pulse-shape effects in nonlinear Thomson scattering, Phys. Rev. A **93**, 063801 (2016).
[53] Note that to make the angular distribution wider and better pronounced these plots were made by choosing both $R, L < \lambda_L$. This, however, is worse for the accuracy of our approximation (see below), so that the figure actually corresponds to a worse scenario.
[54] M. Malakhov, T. Benahmed, E. Gelfer, A. Fedotov, O. Klimo, S. Weber, and S. Rykovanov, Analytical calculation of the spectrum of nonlinear Compton scattering beyond local approximations, arXiv:2606.22427.
[55] D. Seipt and B. Kämpfer, Asymmetries of azimuthal photon distributions in nonlinear Compton scattering in ultrashort intense laser pulses, Phys. Rev. A **88**, 012127 (2013).
[56] Note that the structure of Eq. (28) resembles the notion of a momentum-transfer cross section that typically arises in considerations of momentum transfer in particle collisions.
[57] F. Salehi, M. Le, L. Railing, M. Kolesik, and H. M. Milchberg, Laser-accelerated, low-divergence 15-MeV quasimonoenergetic electron bunches at 1 kHz, Phys. Rev. X **11**, 021055 (2021).
[58] Y.-Y. Chang, J. C. Cabadağ, A. Debus, A. Ghaith, M. LaBerge, R. Pausch, S. Schöbel, P. Ufer, U. Schramm, and A. Irman, Reduction of the electron-beam divergence of laser wakefield accelerators by integrated plasma lenses, Phys. Rev. Appl. **20**, L061001 (2023).
[59] D. Storey, C. Zhang, P. San Miguel Claveria, G. J. Cao, E. Adli, L. Alsberg, R. Ariniello, C. Clarke, S. Corde, T. N. Dalichaouch, *et al.*, Wakefield generation in hydrogen and lithium plasmas at FACET-II: Diagnostics and first beam-plasma interaction results, Phys. Rev. Accel. Beams **27**, 051302 (2024).
[60] V. Yakimenko, S. Meuren, F. Del Gaudio, C. Baumann, A. Fedotov, F. Fiuza, T. Grismayer, M. J. Hogan, A. Pukhov, L. O. Silva, and G. White, Prospect of studying nonperturbative QED with beam-beam collisions, Phys. Rev. Lett. **122**, 190404 (2019).
[61] FACET II beam parameters, https://facet-ii.slac.stanford.edu/facility/beam-parameters.
[62] Y. Shi, D. Blackman, D. Stutman, and A. Arefiev, Generation of ultrarelativistic monoenergetic electron bunches via a synergistic interaction of longitudinal electric and magnetic fields of a twisted laser, Phys. Rev. Lett. **126**, 234801 (2021).
[63] Y. Shi, D. R Blackman, and A. Arefiev, Electron acceleration using twisted laser wavefronts, Plasma Phys. Controlled Fusion **63**, 125032 (2021).
[64] Y. Shi, D. R. Blackman, P. Zhu, and A. Arefiev, Electron pulse train accelerated by a linearly polarized Laguerre–Gaussian laser beam, High Power Laser Sci. Eng. **10**, e45 (2022).
[65] D. R. Blackman, Y. Shi, S. R. Klein, M. Cernaianu, D. Doria, P. Ghenuche, and A. Arefiev, Electron acceleration from transparent targets irradiated by ultra-intense helical laser beams, Commun. Phys. **5**, 116 (2022).
[66] E. Esarey, S. K. Ride, and P. Sprangle, Nonlinear Thomson scattering of intense laser pulses from beams and plasmas, Phys. Rev. E **48**, 3003 (1993).
[67] Note that there is a typo in the expression for α for this case in Ref. [35], where L should be replaced with $L/2$.
[68] For example, for $\omega > \omega_L$ and $R > \lambda_L/2$ the accuracy of Eq. (A4) is better than 6%.

Correction: One of the affiliation indicators for the fifth author was missing at publication and has been inserted.